

NC VERIFICATION OF UP TO 5 AXIS MACHINING PROCESSES USING MANIFOLD STRATIFICATION

Karim Abdel-Malek

Department of Mechanical Engineering and
Center for Computer Aided Design
The University of Iowa
Iowa City, IA 52242
Tel. (319) 335-5676 Fax. (319) 335-5669
karim-abdel-malek@uiowa.edu

Walter Seaman

Department of Mathematics
The University of Iowa
walter-seaman@uiowa.edu

Harn-Jou Yeh

Microtek International
Taiwan
hjyeh@microtek.com.tw

A numerically controlled machining verification method is developed based on a formulation for delineating the volume generated by the motion of a cutting tool on the workpiece (stock). Varieties and subvarieties that are subsets of some Euclidian space defined by the zeros of a finite number of analytic functions are computed and are characterized as closed form equations of surface patches of this volume. The motion of a cutter tool is modeled as a surface undergoing a sweep operation along another geometric entity. A topological space describing the swept volume will be built as a stratified space with corners. Singularities of the variety are loci of points where the Jacobian of the manifold has lower rank than maximal. It is shown that varieties appearing inside the manifold representing the removed material are due to a lower degree strata of the Jacobian. Some of the varieties are complicated and will be shown to be reducible because of their parametrization and are addressed. Benefits of this method are evident in its ability to depict the manifold and to compute a value for the volume.

1. INTRODUCTION

In many applications such as solid modeling, collision detection, and manipulator workspace analyses, it is necessary to determine boundary surfaces to volumes swept by the motion of a geometric entity along another. Computer modeling and simulation used in the validation of numerically controlled (NC) machining programs before they are executed on a computer-controlled machine are known as NC verification.

While recent advances in this field have been made in terms of speed and accuracy, formulations for verifying more than 3 axes machining processes have been very limited. Early work on this subject is due to Wang and Wang (1986). Works addressing the representation of the boundary of the removed material have become of importance in recent years. For example, Boussac and

Crosnier (1996) suggest a representation of swept volumes generated by the motion of deformable objects based on the topological properties of n -dimensional manifolds.

Methods of dual quadtree structures and boundary representation were applied to modeling the parts cut by a wire for Electric Discharge Machining (EDM) verification (Liu and Esterling 1997). The Sweep envelope differential equation method is probably the most elegant method to-date that has been shown to be suitable for NC verification (Blackmore, *et al.* 1997, and Leu, *et al.* 1997). Some of the works that have addressed NC verification but that have not used swept volume methods include Voelker and Hunt (1985), Menon and Voelcker (1992), Oliver and Goodman (1990), Narvekar, *et al.* (1992), Takata, *et al.* (1992), Jerard and Drysdale (1988 and 1991), Koren and Lin (1995), Menon and Robinson (1993), Oliver and Goodman (1990) and Oliver (1990), Narvekar, *et al.* (1992), Liang, *et al.* (1997), and Liu, *et al.* (1996).

The work presented here is a culmination of many reports (Abdel-Malek and Yeh 1997a and 1997b, Abdel-Malek, *et al.* 1997, and Abdel-Malek, *et al.* 1998) and presents them in an integrated and generalized manner. The report by Abdel-Malek and Yeh (1997a) presented the first introduction of the Jacobian rank deficiency method. It was shown to treat consecutive sweep operations of up to four parameters. Further expanding this method, Abdel-Malek, *et al.* (1998) presented a complete rigorous mathematical formulation adapted from kinematics to study the acceleration function on singular surfaces. It was shown that definiteness properties of a quadratic form can play an important role in identifying boundaries that admit no motion and hence are boundaries to the swept volume.

The expansion of this work into a broadly applicable formulation using methods from differential geometry and differential topology are presented in this paper. This is the first introduction of the formulation for n -parameter sweeps where manifold stratification is essential. Furthermore, the adaptation of this work to numerically controlled verification has proven that the formulation is suitable for a variety of fields where sweeping is the underlying action. Manifold stratification and boundary identification are presented in detail.

There have been many works that have treated the topic of swept volumes and the reader is referred to the references surveyed by Abdel-Malek and Yeh (1997a) and by Blackmore, *et al.* 1997. More recent work that have demonstrated analytic methods for computing swept volumes are (Ahn, *et al.* 1997, Elber 1997, Ling and Chase 1996, Sourin and Pasko 1996).

Before proceeding with the analysis and to remain consistent with the terminology used in differential geometry and differential topology (Spivak 1968, Guillemin and Pollack 1974, and Lu, 1976), we define some terms that will be used throughout this work.

Swept volume: The totality of points touched by a geometric entity while in motion.

Variety: Subset of a Euclidean space defined by zeros of a finite number of differentiable functions.

Manifold with singularities: A manifold with singular or boundary parts of lower dimensions: 3, 2, and 1.

Stratified space: A topological space which is built up from lower dimensional pieces that are boundaryless manifolds.

Strata: Plural of the Latin word stratum (layer or level).

Subvariety: Variety that is part of a “reducible” variety.

We shall first present a formulation for characterizing the topological space that is produced as a result of the sweep of a geometric entity (representing the cutting tool) in space along its cutting path due to multiple axes motion. The goal is to identify the boundary to this “manifold with singularities”. Identification of varieties associated with zeros of a finite set of analytic functions will establish a stratified space. These zeros trace a locus of points where the sweep Jacobian has lower rank than maximal and will be shown to comprise varieties. The stratification occurs by studying the locus of points where the Jacobian has a fixed rank. The resulting boundary of the space that is nearly a manifold with singularities will be identified and its volume computed. It will be shown that this formulation allows for an exact computation of the volume, and hence the accuracy of the verification process is very high.

2. FORMULATION

The motion of a cutting tool in an NC milling or EDM process can be characterized as the sweep of a surface (enveloping the tool) along some path. Consider a geometric entity that envelops the cutting tool and is parametrized in terms of one or more variables as a (3×1) vector given by $\Gamma(\mathbf{u})$, where $\mathbf{u} = [u_1 \dots u_n]^T$, and where the tool can be represented as a curve, a surface, or an entity in n -dimensional space. In order to generalize the formulation, we shall also consider boundaries imposed on $\Gamma(\mathbf{u})$ in the form of constraints on the parameters u_i characterized by inequality constraints in the form of $u_i^L \leq u_i \leq u_i^U$. Because of the multi-axis operation of NC machines, the tool surface will be swept several times, each along or about an axis. This path will be considered as a second geometric entity parametrized in terms of one or more variables as a (3×1) vector $\Psi_1(v_1)$. This entity also has a boundary defined by $v_1^L \leq v_1 \leq v_1^U$. The manifold generated by the sweep of $\Gamma(u_1, \dots, u_n)$ on $\Psi_1(v_1)$ is defined by the vector

$$\mathbf{N}_1(\mathbf{q}) = [x(\mathbf{q}) \quad y(\mathbf{q}) \quad z(\mathbf{q})]^T = \mathbf{R}_1(v_1)\Gamma(\mathbf{u}) + \Psi_1(v_1) \quad (1)$$

where $\mathbf{N}_1(\mathbf{q}) = [x \quad y \quad z]^T$ and \mathbf{q} is the vector of *generalized coordinates* defined by $\mathbf{q} = [q_1 \dots q_n]^T = [u_1 \dots u_n \quad v_1]^T$ and $\mathbf{R}_1(v_1)$ is the (3×3) rotation matrix defining the orientation of the cutting tool. In fact, $\mathbf{N}_1(\mathbf{q})$ characterizes the set of all points that belong to the manifold. Another axis motion yields an expanded swept volume in the form of

$$\mathbf{N}_2(\mathbf{q}) = \mathbf{R}_2(v_2)\mathbf{N}_1(\mathbf{q}) + \Psi_2(v_2) = \mathbf{R}_2\mathbf{R}_1\Gamma + \mathbf{R}_2\Psi_1 + \Psi_2 \quad (2)$$

where now $\mathbf{q} = [u_1 \dots u_n \quad v_1 \quad v_2]^T$. Another axis motion yields a modified set defined by

$$\mathbf{N}_3 = \mathbf{R}_3\mathbf{R}_2\mathbf{R}_1\Gamma + \mathbf{R}_3\mathbf{R}_2\Psi_1 + \mathbf{R}_3\Psi_2 + \Psi_3 \quad (3)$$

The generalized case yields a space characterized by the vector function

$\xi = [\xi^{(x)} \quad \xi^{(y)} \quad \xi^{(z)}]^T$, such that

$$\xi(\mathbf{q}) = \prod_{i=1}^{n+m} \mathbf{R}_i \Gamma + \sum_{j=1}^{n+m} \left(\prod_{i=j+1}^{n+m-1} [\mathbf{R}_i] \Psi_j \right) + \Psi_{n+m} \quad (4)$$

where $\mathbf{q} = [\mathbf{u}^T \quad \mathbf{v}^T]^T$, $\mathbf{u} = [u_1 \dots u_n]^T$, and $\mathbf{v} = [v_1 \dots v_m]^T$. The aim is to identify this space, its boundary, and to compute its volume which is material the removed.

To impose inequality constraints, it was shown that a constraint of the form $q_i^{\min} \leq q_i \leq q_i^{\max}$ can be transformed into an equation by introducing a new set of generalized coordinates λ_i such that

$$q_i = a_i + b_i \sin \lambda_i \quad i = 1, \dots, n+m \quad (5)$$

where $a_i = (q_i^{\max} + q_i^{\min})/2$ and $b_i = (q_i^{\max} - q_i^{\min})/2$ are the mid-point and half-range, respectively (Abdel-Malek and Yeh 1997a). At any point in the manifold, a vector constraint equation $\Phi(\mathbf{q}^*)$ with the parametrized inequality constraints can be defined as

$$\Phi(\mathbf{q}^*) = \begin{bmatrix} \xi^{(x)}(\mathbf{q}) - x \\ \xi^{(y)}(\mathbf{q}) - y \\ \xi^{(z)}(\mathbf{q}) - z \\ q_i - a_i - b_i \sin \lambda_i \end{bmatrix} = \mathbf{0} \quad i = 1, \dots, n+m \quad (6)$$

where $\mathbf{q}^* = [\mathbf{u}^T \quad \mathbf{v}^T \quad \boldsymbol{\lambda}^T]^T$ is the vector of all generalized coordinates and $\boldsymbol{\lambda} = [\lambda_1 \quad \dots \quad \lambda_{n+m}]^T$. Note that although $(n+m)$ new variables (λ_i 's) have been added, $(n+m)$ equations have also been added to the constraint vector function without affecting the dimensionality of the problem. In order to have a well-posed formulation; constraints that are used to model the geometry of this problem should be independent, except at certain critical surfaces in the manifold (Implicit Function Theorem) when the Jacobian becomes singular. It is important, therefore, that there not be open sets in the space of the generalized parameters in which the constraints are redundant. Redundancy occurs when the Jacobian $\Phi_{\mathbf{q}^*} = \partial\Phi/\partial\mathbf{q}^*$, is rank-deficient which will subsequently define *varieties* in the manifold.

Candidate varieties forming the boundary of the manifold are identified by computing values that create a locus of points where the Jacobian has lower rank than maximal. The stratification occurs by investigating the locus of points where the Jacobian has a fixed rank.

$$\partial W \subset \left\{ \text{Rank } \Phi_{\mathbf{q}^*}(\mathbf{q}^*) \leq k, \text{ for some } \mathbf{q}^* \text{ with } \Phi(\mathbf{q}^*) = \mathbf{0} \right\} \quad (7)$$

where k is at most $(2n+2m-1)$. This process becomes more pressing as the number of the parameters increases. A manifold with variety or with corners that is built up from lower dimensional pieces is described as a "stratified" space.

Including parameter limits $\Phi(\mathbf{q}(\boldsymbol{\lambda}))$, the rows of $\Phi_{\mathbf{q}}\mathbf{q}_{\boldsymbol{\lambda}} = [\partial\Phi/\partial\mathbf{q}][\partial\mathbf{q}/\partial\boldsymbol{\lambda}]$ are dependent and there exists a set of constants $\mathbf{n}_o = [\gamma_1 \quad \gamma_2 \quad \gamma_3]^T$ that satisfy

$$[\Phi_{\mathbf{q}}\mathbf{q}_{\boldsymbol{\lambda}}]^T \mathbf{n}_o = \mathbf{0} \quad (8)$$

Indeed, \mathbf{n}_o is a vector normal to a tangent plane at a point in the space at which a tangent plane exists and was shown to be normal to a variety (Abdel-Malek and Yeh 1997a). The Jacobian is expanded as

$$\Phi_{\mathbf{q}^*} = \begin{bmatrix} \xi_{q_1}^{(x)} & \xi_{q_2}^{(x)} & \dots & \xi_{q_{n+m}}^{(x)} & 0 & 0 & 0 & 0 \\ \xi_{q_1}^{(y)} & \xi_{q_2}^{(y)} & \dots & \xi_{q_{n+m}}^{(y)} & 0 & 0 & 0 & 0 \\ \xi_{q_1}^{(z)} & \xi_{q_2}^{(z)} & \dots & \xi_{q_{n+m}}^{(z)} & 0 & 0 & 0 & 0 \\ \hline 1 & 0 & 0 & 0 & -b_1 \cos \lambda_1 & 0 & \dots & 0 \\ 0 & 1 & 0 & 0 & 0 & -b_2 \cos \lambda_2 & \dots & 0 \\ 0 & 0 & 1 & 0 & \dots & \dots & \dots & \dots \\ 0 & 0 & 0 & 1 & 0 & 0 & \dots & -b_{n+m} \cos \lambda_{n+m} \end{bmatrix} = \begin{bmatrix} \xi_{\mathbf{q}} & \mathbf{0} \\ \mathbf{I} & \mathbf{q}_\lambda \end{bmatrix} \quad (9)$$

where the notation $\xi_{q_i}^{(x)}$ denotes the partial derivative of $\xi^{(x)}$ with respect to q_i , $\xi_{\mathbf{q}} = \partial \xi / \partial \mathbf{q}$ is the upper left corner sub-matrix (only with respect to \mathbf{q}), $\mathbf{q}_\lambda = \partial \mathbf{q} / \partial \lambda$ is the diagonal lower right corner matrix and \mathbf{I} is the identity matrix.

For an $(n+m)$ -parameter verification, the Jacobian $\Phi_{\mathbf{q}^*}(\mathbf{q}^*)$ row-rank deficiency yields three types of singular behavior.

Criterion (i) In order to make the matrix $\xi_{\mathbf{q}}$ rank deficient of order (d) , it is necessary to determine all *square* sub-Jacobians which are analytic functions. Equating the determinants to zero yields a number of analytic equations to be solved simultaneously. The zeros of the resulting equations are *sets* of constant generalized coordinates denoted by \mathbf{p}_i and are characterized by the following set

$$\mathbf{p}_i = \left\{ \begin{bmatrix} \det(\hat{h}_i \hat{h}_j \hat{h}_k)_1 \\ \vdots \\ \det(\hat{h}_i \hat{h}_j \hat{h}_k)_\eta \end{bmatrix} = \mathbf{0}, \text{ for } i, j, k = 1, \dots, n+m \text{ and } i \neq j \neq k \right\} \quad i = 1, 2, \dots, \beta \quad (10)$$

where \hat{h}_i denotes a column of the matrix $\xi_{\mathbf{q}} = [\hat{h}_1 \dots \hat{h}_m]$, β is the number of singular sets, and \mathbf{p}_i is a subset of \mathbf{q} such that $\mathbf{q}^T = [\mathbf{p}_i^T \quad \mathbf{s}^T]$, i.e., \mathbf{s} contains the remaining non-constant generalized coordinates.

Criterion (ii) If the matrix \mathbf{q}_λ is row-rank deficient (i.e., $b_i \cos \lambda_i$ is zero for some $i = 1, \dots, (n+m)$) then q_i has reached a limit and the corresponding $\xi_{\mathbf{q}}$ is studied for row-rank deficiency. When certain parameters reach their limits, e.g., $[q_i, q_j, q_k] = [q_i^{\text{limit}}, q_j^{\text{limit}}, q_k^{\text{limit}}]$, the corresponding diagonal elements in the matrix \mathbf{q}_λ will be equal to zero. For example, if $q_i = q_i^{\text{min}}$ (or q_i^{max}), the diagonal element of \mathbf{q}_λ will be zero (i.e., $b_i \cos \lambda_i$ is zero for either $i = 1, \dots, 2n$ then q_i has reached a limit). Therefore, the corresponding $\frac{\partial}{\partial \mathbf{q}}[\xi(q_i, \mathbf{q})]$ is subjected

to the rank-deficiency criterion such that the rank of $\Phi_{\mathbf{q}^*}$ will depend on the following matrix

$$\begin{bmatrix} \xi_{q_i} & \dots & \xi_{q_i} & \xi_{q_j} & \xi_{q_k} & \dots & \xi_{q_{n+m}} \\ 0 & \dots & 1 & 0 & 0 & \dots & 0 \\ 0 & \dots & 0 & 1 & 0 & \dots & 0 \\ 0 & \dots & 0 & 0 & 1 & \dots & 0 \end{bmatrix} \quad (11)$$

Solving the rank deficiency condition for Eq. 11 is equivalent to solving the rank deficiency for

$$\left[\xi_{\mathbf{q}} \not\subset [\xi_{q_i}, \xi_{q_j}, \xi_{q_k}] \right], \text{ with } q_i = q_i^{\text{limit}}, q_j = q_j^{\text{limit}}, q_k = q_k^{\text{limit}} \quad (12)$$

where the notation of $\not\subset$ represents the exclusion of the right matrix from the left. Define a new vector $\partial \mathbf{q}^{\text{limit}} = [q_i^{\text{limit}}, q_j^{\text{limit}}, q_k^{\text{limit}}]^T$ which is a sub-vector of \mathbf{q} where $1 \leq \dim(\partial \mathbf{q}^{\text{limit}}) \leq (n-3)$.

Coordinates can be partitioned as $\mathbf{q} = [\mathbf{w}^T, \partial \mathbf{q}^{\text{limit}T}]^T$, and $\mathbf{w} \cap \partial \mathbf{q}^{\text{limit}} = \emptyset$. Then, if $[\xi_{\mathbf{w}}(\mathbf{w}, \partial \mathbf{q}^{\text{limit}})]$ is row rank deficient, the sub-Jacobian $\xi_{\mathbf{q}}$ is also rank deficient. Let the solution for this condition be denoted by $\hat{\mathbf{p}}$, which is a constant sub-vector of \mathbf{w} , and $\mathbf{w} = [\mathbf{u}^T, \hat{\mathbf{p}}^T]^T$. The **type II singularity** set is defined as

$$S^{(2)} \equiv \left\{ \mathbf{p} = [\hat{\mathbf{p}} \cup \partial \mathbf{q}^{\text{limit}}] : \text{Rank}[\xi_{\mathbf{q}}(\mathbf{w}, \partial \mathbf{q}^{\text{limit}})] < 3, \text{ for some } \hat{\mathbf{p}} \in \mathbf{w}, \mathbf{dim}(\partial \mathbf{q}^{\text{limit}}) \leq (n-3) \right\} \quad (13)$$

As for the case of $\dim(\partial \mathbf{q}^{\text{limit}}) = (n-2)$, i.e., only two generalized variables are allowed to vary in their ranges, $\dim(\mathbf{w}) = 2$, and the sub-matrix $\xi_{\mathbf{w}}$ will be of dimension (3×2) , i.e., already row rank deficient. For this case, a **type-III singularity** is defined as

$$S^{(3)} \equiv \left\{ \mathbf{p} \in \mathfrak{R}^{(n+m-2)} : \mathbf{p} \equiv \partial \mathbf{q}^{\text{limit}} = [q_i^{\text{limit}}, q_j^{\text{limit}}, \dots] \right\} \quad (14)$$

Substituting the set \mathbf{p}_i into the vector function $\xi(\mathbf{q})$ yields a variety parametrized in terms of the remainder variables (characterized by \mathbf{s}) as

$$\xi(\mathbf{p}_i, \mathbf{s}) = \xi(\mathbf{s}) \quad (15)$$

subject to the constraints of the generalized coordinates $s_i - a_i - b_i \sin \lambda_i = 0$, where \mathbf{s} is a subset of \mathbf{q} such that $\mathbf{q} = [\mathbf{p}_i^T \quad \mathbf{s}^T]^T$. The vector function of Eq. (15) is a *subvariety of the manifold* whose Jacobian is either full rank or rank deficient. Those that are already rank deficient are identified as *reducible varieties* and can be further stratified. This process is explained below.

3. MANIFOLD STRATIFICATION

The above formulation often yields some surfaces $\in \mathbf{R}^3$ with a parameterization of three variables and are rank deficient. This indicates that the parameterization is not one-to-one and that, as can be readily shown, the Jacobian of these entities is already rank deficient.

Since the rank-deficiency of this variety is of order one, it yields two constant generalized coordinates, i.e., one-parameter geometric entities. Curves instead of surfaces that identify the boundary are determined. For this case when $\xi_i(\mathbf{s}_i) : \mathbf{s}_i(\epsilon) \in \mathfrak{R}^3 \rightarrow \mathfrak{R}^3$, where ϵ is the corresponding vector of slack variables $\epsilon = [\lambda_k \quad \lambda_\ell \quad \lambda_m]^T$, the Jacobian of the variety is

$$\xi_\epsilon = \xi_{\mathbf{s}} \mathbf{s}_\epsilon \quad (16)$$

For a parameter at its limit (q_i^{limit}), the second block matrix of Eq. (16) is rank deficient. An elementary matrix of row operations \mathbf{E}_i applied to $[\mathbf{s}_\epsilon]$ yields a row echelon form such that

$$\mathbf{E}_i[\mathbf{s}_\epsilon] = \mathbf{E}_{RE} \quad (17)$$

where $\mathbf{E}_1 = \begin{bmatrix} 0 & 1 & 0 \\ 0 & 0 & 1 \\ 0 & 0 & 0 \end{bmatrix}$, $\mathbf{E}_2 = \begin{bmatrix} 1 & 0 & 0 \\ 0 & 0 & 1 \\ 0 & 0 & 0 \end{bmatrix}$, and $\mathbf{E}_3 = \begin{bmatrix} 1 & 0 & 0 \\ 0 & 1 & 0 \\ 0 & 0 & 0 \end{bmatrix}$; where the subscript denotes the

parameter number, and \mathbf{E}_{RE} is a row echelon form. This same matrix applied to $[\xi_s]^T$ yields

$$\mathbf{E}_i[\xi_s]^T = \begin{bmatrix} \Lambda \\ \mathbf{0} \end{bmatrix} \quad (18)$$

where

$$[\Lambda] = [\Lambda_1 \quad \Lambda_2 \quad \Lambda_3] \quad (19)$$

where $\dim(\Lambda) = (2 \times 3)$ and $\dim(\Lambda_j) = (2 \times 1)$ for $j = 1, 2, 3$. The rank deficiency condition is applied again to $[\Lambda]$. Solutions to the three equations are singular sets denoted by γ_i such that

$$\gamma_i = \left\{ \begin{bmatrix} D_1 \\ D_2 \\ D_3 \end{bmatrix} = \mathbf{0}, \text{ for } \gamma_i \in \mathbf{s}, \gamma_i \cap \beta_i = \phi \right\} \quad (20)$$

where $D_1 = |\Lambda_1 \Lambda_2|$, $D_2 = |\Lambda_2 \Lambda_3|$, and $D_3 = |\Lambda_1 \Lambda_3|$ subject to the parameter constraints and where γ_i is a subset of \mathbf{s} such that $\mathbf{s}_i^T = [\gamma_i^T \quad \beta_i]$, where β_i is the remaining variable such that

$$\xi_i(\gamma_i, \beta_i) = \kappa_i(\beta_i) \quad (21)$$

where $\kappa_i(\beta_i)$ is a parametric space curve and $\dim(\kappa(\beta)) = (3 \times 1)$ which represent boundary curves to the variety $\xi(\mathbf{s})$. This submanifold is characterized by the varieties $\xi(\mathbf{s})$ subject to $\kappa(\beta)$. Determination of the boundary to the manifold is addressed in the following section.

4. BOUNDARY VARIETIES

In order to distinguish regions of a variety that are part of boundary of the manifold, a second-order criterion is introduced. The Jacobian is not enough but it will be shown that a form of the Hessian will identify such a boundary. Consider a point P on a smooth variety with a known vector normal (note that this is only possible because of the capability of this formulation to obtain closed form equations of the varieties). This point may admit motion in either normal direction to the variety. This motion depends on the difference between the component of acceleration in the normal direction and the centripetal acceleration due to its tangential velocity. An indicator characterizes the difference (which is true for the general motion of a particle on a curve or surface (Abdel-Malek, *et al.* 1998)), such that

$$\eta_p = \eta_p(H) = a_n - \frac{v_t^2}{\rho_o} \quad (22)$$

where v_t is the tangential velocity, a_n is the component of acceleration in the normal direction to the variety, and $1/\rho_o$ is the normal curvature of the variety *with respect to the tangent direction* of v_t (ρ_o is the radius of curvature). At a boundary, η_p will only indicate motion towards the interior of the manifold. It will be shown that these boundaries do not admit motion regardless of the values of velocity or acceleration at the point of interest, but will only depend on the definiteness properties of a quadratic form.

In order to apply Eq. 22 to varieties $\xi(\mathbf{s})$, we define the *Time-Modified First and Second Fundamental Forms* (Farin 1993), denoted by \mathbf{I}'_p and \mathbf{II}'_p , respectively,

$$\mathbf{I}'_p \equiv \dot{\mathbf{s}}^T \xi_s^T \xi_s \dot{\mathbf{s}} \quad (23)$$

$$\mathbf{II}'_p \equiv \dot{\mathbf{s}}^T [\mathbf{n}^T \xi]_{ss} \dot{\mathbf{s}} \quad (24)$$

such that the normal curvature is still defined by $K_o = 1/\rho_o = \mathbf{II}'_p/\mathbf{I}'_p$ (note that fundamental forms are extensively used in differential geometry (Farin 1993)). In general, the tangential velocity in terms of ξ or Φ at any point on the surface is

$$\mathbf{v}_t = \xi_s \dot{\mathbf{s}} = \Phi_q \dot{\mathbf{q}} \quad (25)$$

where $\dot{\mathbf{q}} = \mathbf{q}_\lambda \dot{\lambda}$. The squared norm of the velocity is $|\mathbf{v}_t|^2 = \mathbf{v}_t^T \mathbf{v}_t = \dot{\mathbf{s}}^T \xi_s^T \xi_s \dot{\mathbf{s}}$ which is equal to the Time-Modified First Fundamental Form \mathbf{I}'_p . Therefore, \mathbf{I}'_p can be written as $\mathbf{I}'_p = |\mathbf{v}_t|^2$. Substituting for $1/\rho_o$ and for \mathbf{I}'_p into η yields

$$\eta = a_n - |\mathbf{v}_t|^2 (\mathbf{II}'_p/\mathbf{I}'_p) = a_n - \mathbf{II}'_p \quad (26)$$

which indicates that time-modified second fundamental form is indeed the centripetal acceleration for a point on a variety. We will first evaluate an expression for \mathbf{II}'_p , followed by an expression for a_n to obtain the indicator η .

4.1 Determining the Centripetal acceleration

Since a_n is in terms of $\dot{\mathbf{q}}$ and to express \mathbf{II}'_p in terms of $\dot{\mathbf{q}}$, the velocity vector ($\dot{\mathbf{s}}$) on a variety is extracted from Eq. 25. Since ξ_s is not square, a generalized inverse can be written such that

$$\dot{\mathbf{s}} = \mathbf{B} \Phi_q \dot{\mathbf{q}} = \mathbf{B} \Phi_q \mathbf{q}_\lambda \dot{\lambda} \quad (27)$$

where \mathbf{B} is the generalized inverse defined by $\mathbf{B} = [\mathbf{E} \xi_s^T]^{-1} \mathbf{E}$ and $\mathbf{E} = \begin{bmatrix} 1 & 0 & 0 \\ 0 & 1 & 0 \end{bmatrix}$ if the first and second rows of ξ_s are independent, $\mathbf{E} = \begin{bmatrix} 1 & 0 & 0 \\ 0 & 0 & 1 \end{bmatrix}$ if the first and third rows are independent and $\mathbf{E} = \begin{bmatrix} 0 & 1 & 0 \\ 0 & 0 & 1 \end{bmatrix}$ if the second and third rows are independent. Substituting the expression for $\dot{\mathbf{s}}$ into Eq. 24 yields

$$\mathbf{II}'_p = \dot{\mathbf{s}}^T [\mathbf{n}^T \xi]_{ss} \dot{\mathbf{s}} = \dot{\lambda}^T \mathbf{q}_\lambda \Phi_q \mathbf{B}^T [\mathbf{n}^T \xi]_{ss} \mathbf{B} \Phi_q \mathbf{q}_\lambda \dot{\lambda} \quad (28)$$

which is a general expression for \mathbf{II}'_p .

4.2 Determining the Component of Normal Acceleration

Differentiating Eq. 25 again with respect to time and using indicial form, the acceleration at any point is

$$\ddot{\xi}_i = \frac{d}{dt} \left[\frac{d\Phi_i}{dq_j} \frac{dq_j}{d\lambda_k} \dot{\lambda}_k \right] + \left[\frac{d\Phi_i}{dq_j} \right] \frac{d}{dt} \left(\frac{dq_j}{d\lambda_k} \right) \dot{\lambda}_k + \left[\frac{d\Phi_i}{dq_j} \right] \frac{dq_j}{d\lambda_k} \ddot{\lambda}_k \quad (29)$$

Expanding the derivatives and collecting similar terms yields

$$\ddot{\xi}_i = \dot{\lambda}_n \left\{ \frac{dq_j}{d\lambda_n} \left[\frac{d^2\Phi_i}{dq_m dq_j} \right] \frac{dq_j}{d\lambda_k} + \frac{d\Phi_i}{dq_j} \frac{d^2q_j}{d\lambda_n d\lambda_k} \right\} \dot{\lambda}_k + \left[\frac{d\Phi_i}{dq_j} \frac{dq_j}{d\lambda_k} \right] \ddot{\lambda}_k \quad (30)$$

In matrix form, Eq. 30 is written as

$$\ddot{\xi} = \dot{\lambda} \left\{ \mathbf{q}_\lambda^T \Phi_{qq} \mathbf{q}_\lambda + \sum_{i=1}^{n+m} \frac{d\Phi}{dq_i} \cdot [q_i]_{\lambda\lambda} \right\} \dot{\lambda} + [\Phi_q \mathbf{q}_\lambda] \ddot{\lambda} \quad (31)$$

To obtain the normal acceleration, $\ddot{\xi}$ is projected onto \mathbf{n}_o . Recall that \mathbf{n}_o is a vector normal to the variety. Multiplying both sides of Eq. 31 by the vector \mathbf{n}_o^T eliminates the last term of the right hand side (definition of the normal as the basis of the null space in Eq. 8).

The component of the normal acceleration is then

$$a_n = \mathbf{n}_o^T \ddot{\xi} = \dot{\lambda}^T \mathbf{H}^* \dot{\lambda} \quad (32)$$

where

$$\mathbf{H}^*(\mathbf{q}_o, \lambda_o) = \mathbf{q}_\lambda^T [\mathbf{n}_o^T \Phi]_{qq} \mathbf{q}_\lambda + \sum_{i=1}^n \frac{d(\mathbf{n}_o^T \Phi)}{dq_i} \cdot [q_i]_{\lambda\lambda} \quad (33)$$

4.3 A Form of the Hessian Matrix

To compute a value for the indicator (η), substitute for a_n (from Eq. 33) and for \mathbf{II}'_p (from Eq. 28) into Eq. 26, such that

$$\eta = a_n - \mathbf{II}'_p = \dot{\lambda}^T \mathbf{Q}^* \dot{\lambda} \quad (34)$$

where

$$\mathbf{Q}^* = \mathbf{H}^* - \mathbf{q}_\lambda^T \Phi_q^T \mathbf{B}^T [\mathbf{n}^T \xi]_{ss} \mathbf{B} \Phi_q \mathbf{q}_\lambda \quad (35)$$

where \mathbf{Q}^* is the quadratic matrix. Definiteness properties of the quadratic form of Eq. 35 determines whether a variety admits motion in the direction of \mathbf{n}^T at a specified point (i.e., independent of the value of $\dot{\lambda}$). This form will indicate if a region on a variety is a part of the boundary of the manifold, or is boundary to a void since no motion will be admitted in the direction of the exterior of the manifold (including voids). If \mathbf{Q}^* is indefinite, the variety admits motion along either normal direction and is not a boundary.

For the case when $q_i = q_i^{\text{limit}}$ (at the boundary of a sweep or at the boundary of an entity), Eq. 35 yields a semi-definite quadratic form. For this case, we propose the projection of a variational movement $\delta\Phi = \Phi_{q_i} \delta q_i$ due to δq_i onto the normal direction \mathbf{n} such that the normal component is given by

$$\sigma = \mathbf{n}^T \Phi_{q_i} \delta q_i \quad (36)$$

where δq_i is a specified magnitude of ± 1 as follows

$$\delta q_i = \begin{cases} +1 & \text{if } q_i \text{ is at lower bound} \\ -1 & \text{if } q_i \text{ is at upper bound} \end{cases} \quad (37)$$

Positive values of σ in Eq. 36 indicate that the variety can admit motion in the positive direction of \mathbf{n} . A boundary is established when an enclosure is identified as having admissible output directions for all points on its boundary directed towards the interior of that enclosure as illustrated in Fig. 1. A void is identified as an enclosure that exhibits admissible directions towards the exterior of the manifold. The algorithm is presented in Appendix A.

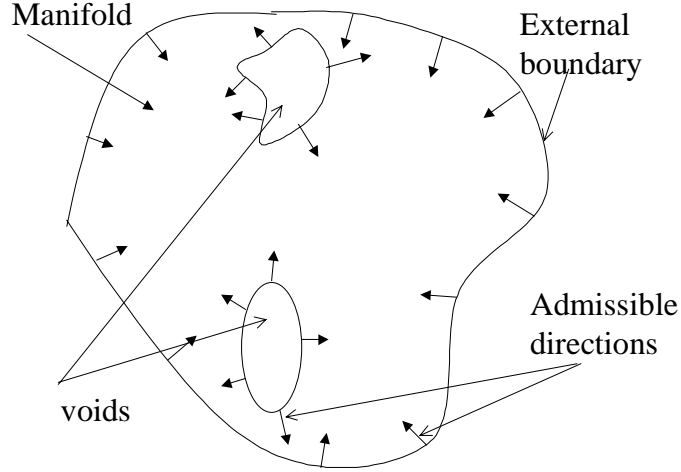


Fig. 1 Identifying the boundary using admissible directions

5. AN INTRODUCTORY EXAMPLE

Consider the NC verification of a process involving the motion of a cutting tool represented by a cylindrical surface (two parameters) along a cutting path (a curve of one parameter) to generate a manifold in three parameters. The cylindrical surface is given by

$$\Gamma(\mathbf{u}) = [10\cos u_2 \quad -20 - u_1 \quad 10\sin u_2]^T \quad (38)$$

with the following geometric constraints $0 \leq u_1 \leq 20$ and $0 \leq u_2 \leq 2\pi$. The orientation of the

motion is defined by the matrix $\mathbf{R}(v_1) = \begin{bmatrix} \cos v_1 & -\sin v_1 & 0 \\ 0 & 0 & -1 \\ \sin v_1 & \cos v_1 & 0 \end{bmatrix}$ subject to $\pi/4 \leq v_1 \leq 5\pi/4$ and

$\Psi(v_1) = [0 \quad 0 \quad 0]^T$. The manifold is characterized by 3 parameters

$$\xi(\mathbf{q}) = \begin{bmatrix} 10\cos q_3 \cos q_5 + 20\sin q_3 + q_4 \sin q_3 \\ -10\sin q_5 \\ -20\cos q_3 - q_4 \cos q_3 + 10\cos q_5 \sin q_3 \end{bmatrix} \quad (39)$$

where $\mathbf{q} = [q_3 \quad q_4 \quad q_5]^T$. Note that we have used the indices 3, 4, and 5 in order to simplify the continuation of this example in the following section. The limits are parametrized as $q_3 = (3\pi/4) + (\pi/2)\sin \lambda_3$, $q_4 = 10 + 10\sin \lambda_4$, and $q_5 = \pi + \pi\sin \lambda_5$. The boundary to $\xi(\mathbf{q})$ is to be determined. The Jacobian is computed as the matrix

$$\Phi_{\mathbf{q}} = \begin{bmatrix} 20\cos q_3 + q_4 \cos q_3 - 10\cos q_5 \sin q_3 & \sin q_3 & -10\cos q_3 \sin q_5 & 0 & 0 & 0 \\ 0 & 0 & -10\cos q_5 & 0 & 0 & 0 \\ 10\cos q_3 \cos q_5 + 20\sin q_3 + q_4 \sin q_3 & -\cos q_3 & -10\sin q_3 \sin q_5 & 0 & 0 & 0 \\ 1 & 0 & 0 & -(\pi/2)\cos \lambda_3 & 0 & 0 \\ 0 & 1 & 0 & 0 & -10\cos \lambda_4 & 0 \\ 0 & 0 & 1 & 0 & 0 & -\pi \cos \lambda_5 \end{bmatrix}$$

The criteria are applied to the upper (3×3) corner matrix $\xi_{\mathbf{q}}$ which is square. Therefore, the rank-deficiency criteria are applied by computing the zeros of the determinant of $\xi_{\mathbf{q}}$ as

$$|\xi_{\mathbf{q}}| = -10(20(\cos q_3)^2 \cos q_5 + q_4(\cos q_3)^2 \cos q_5 (\sin q_3)^2 + q_4 \cos q_5 (\sin q_3)^2) = 0 \quad (40)$$

which can be simplified to $|\xi_q| = -10(20 + q_4) \cos q_5 = 0$. Solutions that satisfy $|\xi_q| = 0$ are $\cos q_5 = 0$, (i.e., $q_5 = 3\pi/2$, $q_5 = \pi/2$) and $q_4 = -20$. Only $\mathbf{p}_1 = \{q_5 = 3\pi/2\}$, and $\mathbf{p}_2 = \{q_5 = \pi/2\}$ are considered since they satisfy the inequality constraints.

Rank deficiency conditions imposed on the matrix \mathbf{q}_λ yield five other singularities as $\mathbf{p}_3 = \{q_3 = \pi/4\}$, $\mathbf{p}_4 = \{q_3 = 5\pi/4\}$, $\mathbf{p}_5 = \{q_4 = 0\}$, $\mathbf{p}_6 = \{q_4 = 20\}$, and $\mathbf{p}_7 = \{q_5 = 0\}$. Substituting these singularities into Eq. (39) yields parametric equations of varieties. For example, substituting $\mathbf{p}_2 = \{q_5 = \pi/2\}$ into Eq. (39) yields the following variety

$$\xi(\mathbf{s}_2) = [20 \sin q_3 + q_4 \sin q_3 \quad -10 \quad -20 \cos q_3 - q_4 \cos q_3]^T \quad (41)$$

where $\mathbf{s}_2 = [q_3 \quad q_4]^T$. Similarly, for $\mathbf{p}_1 = \{q_3 = 5\pi/4\}$, the equation is generated and varieties for both \mathbf{p}_1 and \mathbf{p}_2 are shown in Fig. 2a. Varieties due to \mathbf{p}_3 and \mathbf{p}_4 are shown in Fig. 2b and those due to \mathbf{p}_6 and \mathbf{p}_7 are shown in Fig. 2c (Note that varieties are shown using Mathematica[®] using the parametric plot 3D capabilities).

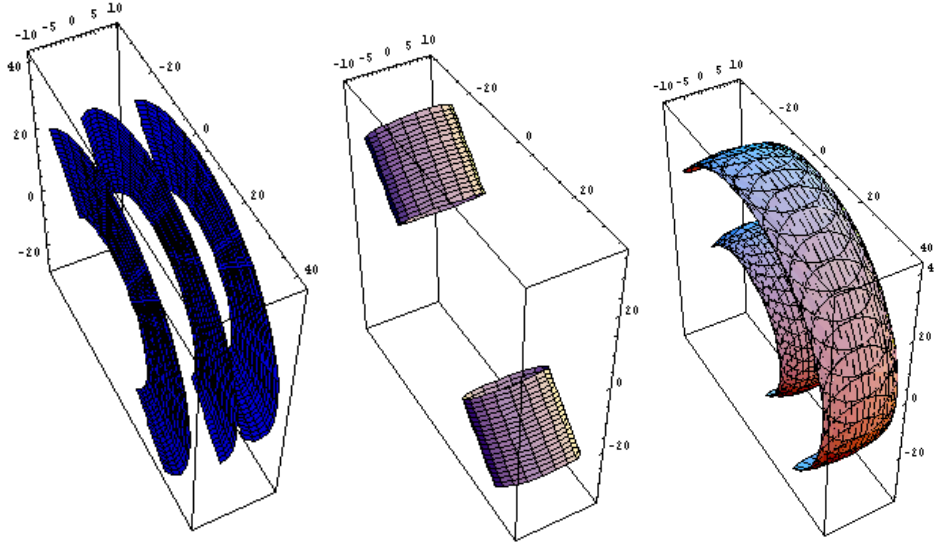


Fig. 2 Varieties due to (a) \mathbf{p}_1 , \mathbf{p}_2 , \mathbf{p}_7 (b) \mathbf{p}_3 , \mathbf{p}_4 and (c) \mathbf{p}_5 , \mathbf{p}_6

Boundary Identification: Consider the variety due to \mathbf{p}_6 where $\mathbf{u}_6 = [q_3 \quad q_5]^T$. For a point on this variety at $\mathbf{q}_o = [3\pi/4 \quad q_4^U \quad \pi]^T$. Evaluating the normal \mathbf{n}_o from the basis of the null space

of $[\Phi_q \mathbf{q}_\lambda]^T = \begin{bmatrix} -33.3 & 0 & 55.5 \\ 0 & 0 & 0 \\ 0 & 31.4 & 0 \end{bmatrix}$ at \mathbf{q}_o yields the normal $\mathbf{n}_o = [0.857 \quad 0 \quad 0.514]^T$. The matrix

$(\mathbf{q}_\lambda \Phi_{qq} \mathbf{q}_\lambda)^T = \begin{bmatrix} -101.6 & 0 & 0 \\ 0 & 0 & 0 \\ 0 & 0 & -23.9 \end{bmatrix}$, and the matrix is chosen as $\mathbf{E} = \begin{bmatrix} 1 & 0 & 0 \\ 0 & 0 & 1 \end{bmatrix}$, and

$\mathbf{B} = [\mathbf{E} \xi_u]^{-1} \mathbf{E} = \begin{bmatrix} 0 & 0 & 0 \\ 0 & 0.1 & 0 \end{bmatrix}$. The matrix \mathbf{Q}^* of the quadratic form is evaluated as

$$\mathbf{Q}^* = \begin{bmatrix} 0 & 0 & 0 \\ 0 & -9.69 & 0 \\ 0 & 0 & 0 \end{bmatrix}$$

The eigenvalues of \mathbf{Q}^* are evaluated as $\{-9.69, 0, 0\}$, which indicates a negative semi-definite quadratic form. Since q_4 is at its upper bound (q_4^U), the additional value of σ is evaluated with $\delta q_4 = -1$. The value for $\sigma = \mathbf{n}^T \Phi_{q_4} \delta q_4 = -0.97$. Since the sign of σ is the same as that of the eigenvalues of \mathbf{Q}^* , it indicates that the surface ξ_6 at \mathbf{q}_o only admits motion in the opposite direction of the normal \mathbf{n}_o (towards the interior of the manifold).

Consider now the cylindrical surface at the start of the sweep operation with $\mathbf{p}_3 = \{q_3 = \pi/4\}$ at $\mathbf{q}_o = \{q_3^L, q_4 = 10, q_5 = \pi\}$ as shown in Fig. 3, the eigenvalues are $\{-195.2, -47.12, -0.6\}$ and therefore, no motion towards the exterior occurs.

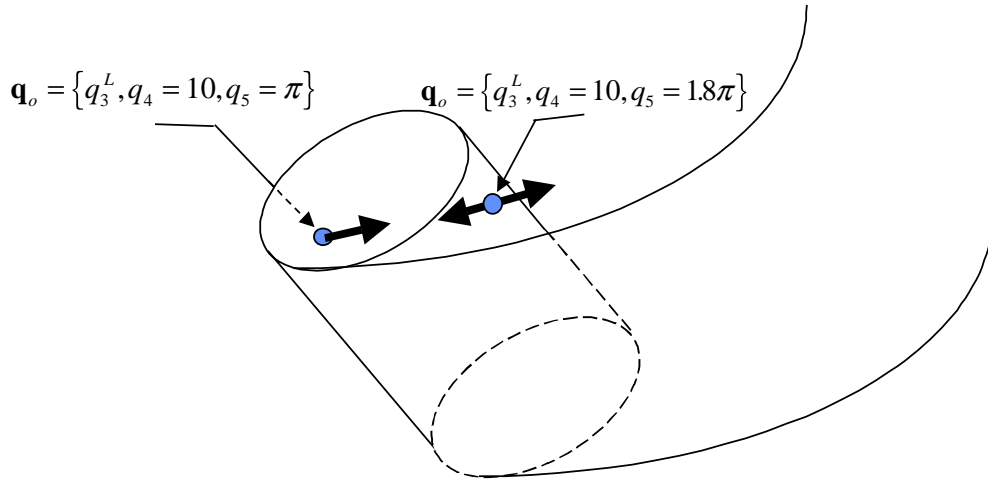


Fig. 3 The variety ξ_3

However, on that same surface, at the opposite side at $\mathbf{q}_o = \{q_3^L, q_4 = 10, q_5 = 1.8\pi\}$, the eigenvalues are $\{37.9, 0.027, 0\}$ which is an indefinite form. The indicator $\sigma = -24.18$ is different in sign from the nonzero eigenvalues, therefore admitting motion; i.e., this surface, although it does not admit motion along some regions, it does on another region interior to the manifold. The complete boundary to the manifold is identified and shown in Fig. 4.

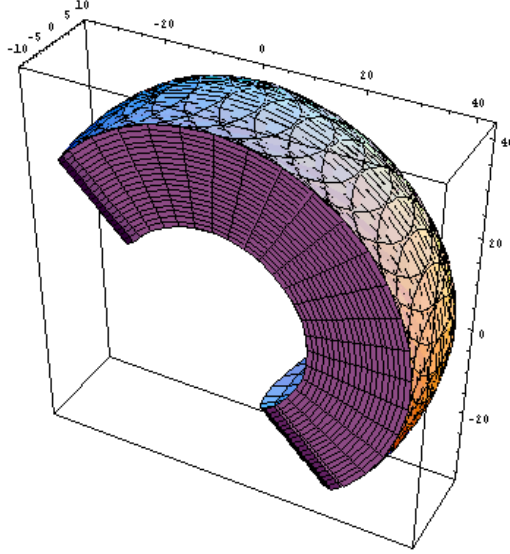


Fig. 4 Volume removed

6. FIVE-PARAMETER NC VERIFICATION

Consider the motion of the same cutting tool represented in the introductory example by a cylindrical surface such that a 5-parameter verification will be developed. The machining operation will sweep the cylindrical surface first along the curve given above to yield the accessible set now called Γ (Eq. 39) such that

$$\Gamma(q_3, q_4, q_5) = \begin{bmatrix} 10\cos q_3 \cos q_5 + 20\sin q_3 + q_4 \sin q_3 \\ -10\sin q_5 \\ -20\cos q_3 - q_4 \cos q_3 + 10\cos q_5 \sin q_3 \end{bmatrix} \quad (42)$$

The first will be a rotational motion of Γ and the second will be a translation along an axis. The result is a sweep of Γ along a cylindrical surface defined by the rotation matrix

$$\mathbf{R}(q_2) = \begin{bmatrix} \cos q_2 & -\sin q_2 & 0 \\ \sin q_2 & \cos q_2 & 0 \\ 0 & 0 & 1 \end{bmatrix} \text{ and } \Psi = [0 \ 0 \ 0]^T \quad (43)$$

followed by a translation with $\mathbf{R}(q_1) = \mathbf{I}$ and $\Psi(q_1) = [0 \ 0 \ 30 + q_1]^T$ subject to the following constraints $0 \leq q_1 \leq 20$, $\pi/4 \leq q_2 \leq 7\pi/4$, $\pi/4 \leq q_3 \leq 5\pi/4$, $0 \leq q_4 \leq 20$, and $0 \leq q_5 \leq 2\pi$. The totality of points characterizing the manifold is given by the vector function

$$\xi(\mathbf{q}) = \begin{bmatrix} 10\cos q_2 \cos q_3 \cos q_5 + 10\sin q_2 \sin q_5 + 20\cos q_2 \sin q_3 + q_4 \cos q_2 \sin q_3 \\ 10\sin q_2 \cos q_3 \cos q_5 - 10\cos q_2 \sin q_5 + 20\sin q_2 \sin q_3 + q_4 \sin q_2 \sin q_3 \\ 10\sin q_3 \cos q_5 - 20\cos q_3 - q_4 \cos q_3 + 30 + q_1 \end{bmatrix} \quad (44)$$

where $\mathbf{q} = [q_1 \ q_2 \ q_3 \ q_4 \ q_5]^T$. The (3×5) upper sub-Jacobian of $\xi_{\mathbf{q}}$ is computed as

$$\xi_{\mathbf{q}} = \begin{bmatrix} 0 & -10\sin q_2 \cos q_3 \cos q_5 + 10\cos q_2 \sin q_5 - 20\sin q_2 \sin q_3 - q_4 \sin q_2 \sin q_3 \\ 0 & 10\cos q_2 \cos q_3 \cos q_5 + 10\sin q_2 \sin q_5 + 20\cos q_2 \sin q_3 + q_4 \cos q_2 \sin q_3 \\ 1 & 0 \end{bmatrix}$$

$$\left. \begin{array}{ccc} -10\cos q_2 \sin q_3 \cos q_5 + 20\cos q_2 \cos q_3 + q_4 \cos q_2 \cos q_3 & \cos q_2 \sin q_3 & -10\cos q_2 \cos q_3 \sin q_5 + 10\sin q_2 \cos q_5 \\ -10\sin q_2 \sin q_3 \cos q_5 + 20\sin q_2 \cos q_3 + q_4 \sin q_2 \cos q_3 & \sin q_2 \sin q_3 & -10\sin q_2 \cos q_3 \sin q_5 - 10\cos q_2 \cos q_5 \\ 10\cos q_3 \cos q_5 + 20\sin q_3 + q_4 \sin q_3 & -\cos q_3 & -10\sin q_3 \sin q_5 \end{array} \right] \quad (45)$$

and the lower corner matrix is

$$\mathbf{q}_\lambda(\lambda) = \begin{bmatrix} -10\cos \lambda_1 & 0 & 0 & 0 & 0 \\ 0 & -(3\pi/4)\cos \lambda_2 & 0 & 0 & 0 \\ 0 & 0 & (\pi/2)\cos \lambda_3 & 0 & 0 \\ 0 & 0 & 0 & 10\cos \lambda_4 & 0 \\ 0 & 0 & 0 & 0 & \pi \cos \lambda_5 \end{bmatrix} \quad (46)$$

Criterion (i): Since $(n+m) = 5$ and $\dim(\xi_{\mathbf{q}}) = 3 \times 5$, there are ten (3×3) square sub-Jacobians whose analytic determinants need to be determined. The resulting nonlinear equations are as follows.

$$\begin{aligned} |j1| &= -q_4^2 \sin q_3 \cos q_3 + 100\cos q_3 (\cos q_5)^2 \sin q_3 + 200\cos q_5 - 40q_4 \sin q_3 \cos q_3 \\ &\quad - 400(\cos q_3)^2 \cos q_5 - 400\sin q_3 \cos q_3 + 10q_4 \cos q_5 - 20q_4 (\cos q_3)^2 \cos q_5 = 0 \\ |j2| &= -10\sin q_3 \cos q_3 \cos q_5 - 20 + 20(\cos q_3)^2 - q_4 (\cos q_3)^2 = 0 \\ |j3| &= 100(\cos q_3)^2 \cos q_5 \sin q_5 + 200\sin q_3 \cos q_3 \sin q_5 + 10q_4 \sin q_3 \cos q_3 \sin q_5 - 100q_4 \cos q_5 \sin q_5 = 0 \\ |j4| &= 0 \quad \text{and} \quad |j5| = 100(\cos q_5)^2 \sin q_3 - 200\cos q_3 \cos q_5 - 10q_4 \cos q_5 \cos q_3 = 0 \\ |j6| &= -10\sin q_3 \cos q_5 = 0 \quad \text{and} \quad |j7| = 400\sin q_3 + 10q_4 \cos q_5 \cos q_3 + 200\cos q_3 \cos q_5 + 40q_4 \sin q_3 + q_4^2 \sin q_3 = 0 \\ |j8| &= 0 \quad \text{and} \quad |j9| = 10q_4 \sin q_5 \sin q_3 + 200\sin q_3 \sin q_5 = 0 \quad \text{and} \quad |j10| = -200\cos q_5 - 10q_4 \cos q_5 = 0 \end{aligned}$$

Zeros of the above ten equations that satisfy the constraint equations are the sets given by $\mathbf{p}_1 = \{q_3 = \pi, q_5 = \pi/2\}$ and $\mathbf{p}_2 = \{q_3 = \pi, q_5 = 3\pi/2\}$.

Criterion (ii): The lower right corner matrix of \mathbf{q}_λ is rank deficient at $q_2 = \pi/4$. Substituting $q_2 = \pi/4$ into $\xi(\mathbf{q})$ and computing the Jacobian subject to the rank-deficiency condition yields the singular sets $\mathbf{p}_3 = \{q_2 = \pi/4, q_5 = \pi/2\}$, and $\mathbf{p}_4 = \{q_2 = \pi/4, q_5 = 3\pi/2\}$. Similarly, substituting each constraint limit and applying the rank-deficiency yields 50 other singular sets some of which are $\mathbf{p}_5 = \{q_2 = 7\pi/4, q_5 = 3\pi/2\}$, $\mathbf{p}_6 = \{q_2 = 7\pi/4, q_5 = 3\pi/2\}$, and $\mathbf{p}_{26} = \{q_1 = 20, q_3 = 5\pi/4, q_5 = \pi\}$, $\mathbf{p}_{27} = \{q_1 = 0, q_4 = 0\}$, $\mathbf{p}_{28} = \{q_1 = 0, q_4 = 20\}$, $\mathbf{p}_{29} = \{q_1 = 20, q_4 = 0\}$, and $\mathbf{p}_{30} = \{q_1 = 20, q_4 = 20\}$.

Note that the set \mathbf{p}_{27} , for example, will have its corresponding \mathbf{s}_{27} , with $\dim(\mathbf{s}_{27}) = 3$ which identifies a reducible variety.

Substituting the sets \mathbf{p}_i into the accessible set (Eq. 44) yields varieties parametrized in two variables and can readily be depicted. Fig. 5 depicts a number of varieties.

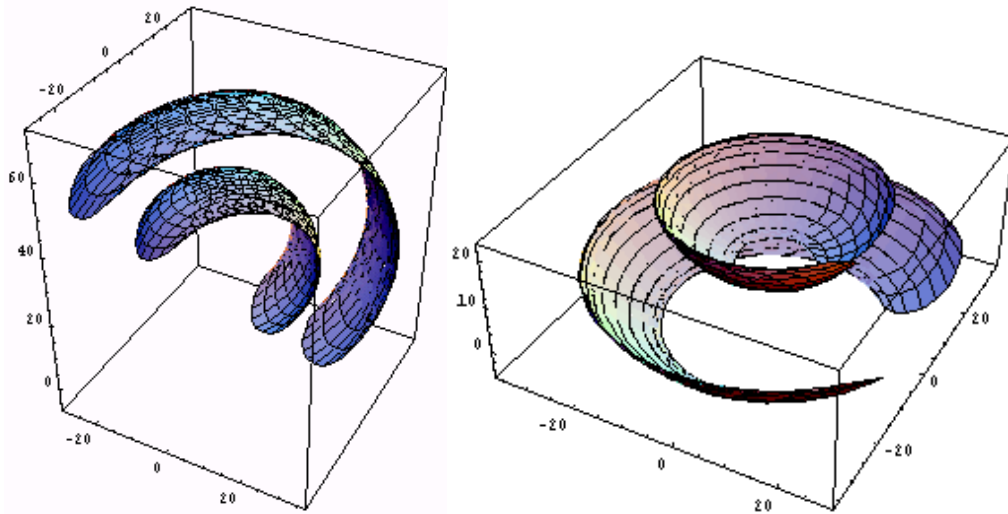


Fig. 5. Varieties due to (a) $\mathbf{p}_{63}, \mathbf{p}_{65}$ (b) $\mathbf{p}_{71}, \mathbf{p}_{72}$

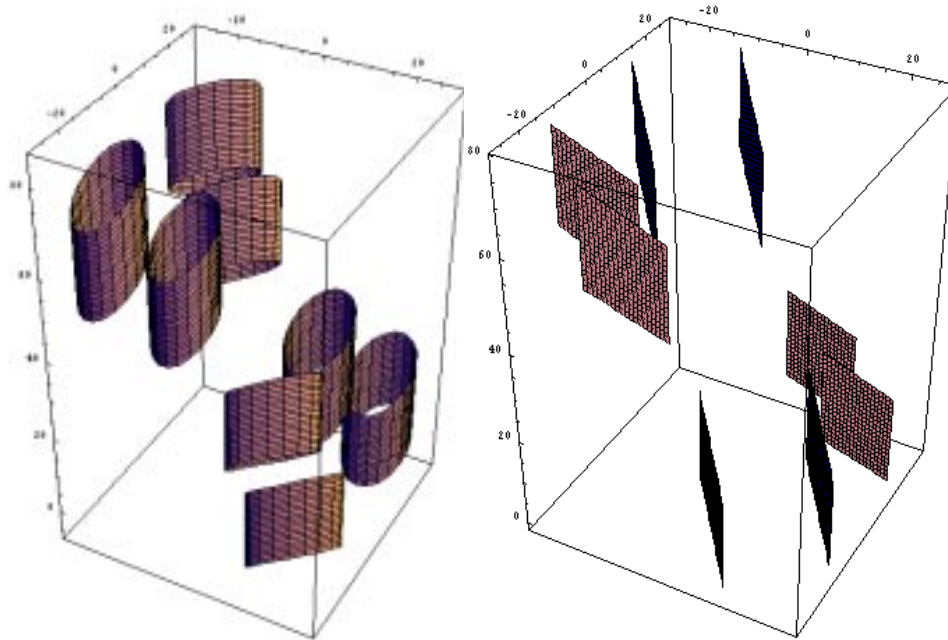


Fig. 5. Varieties due to (c) $\mathbf{p}_{79} - \mathbf{p}_{86}$ and (d) $\mathbf{p}_{31} - \mathbf{p}_{38}$

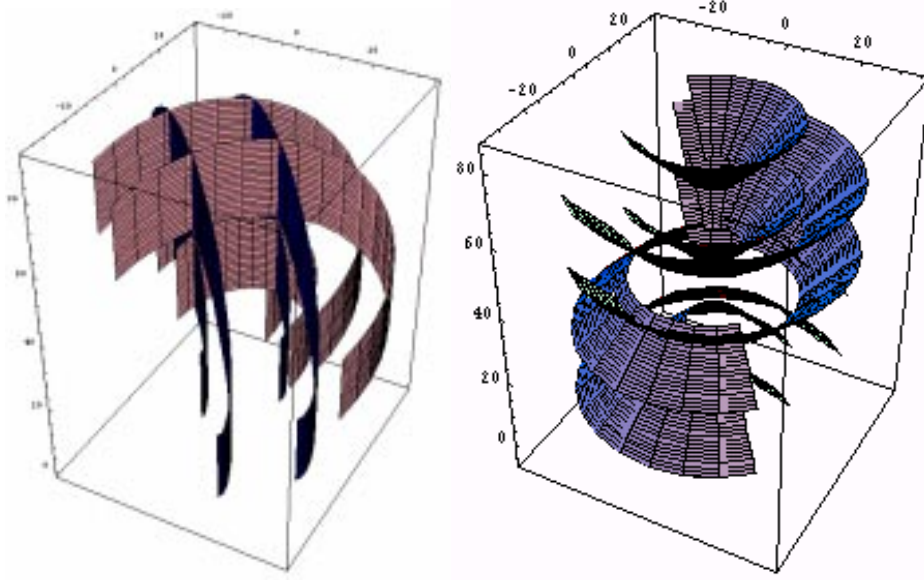


Fig. 5. Varieties due to (e) $\mathbf{p}_{39} - \mathbf{p}_{46}$ and (f) $\mathbf{p}_{33} \dots \mathbf{p}_{27}$

Reducible Varieties: To illustrate, substitute the set $\mathbf{p}_{27} = \{q_1 = 0, q_4 = 0\}$ into $\xi(\mathbf{q})$ yields

$$\xi_{27}(\mathbf{s}_{27}) = \begin{bmatrix} 10 \cos q_2 \cos q_3 \cos q_5 + 10 \sin q_2 \sin q_5 + 20 \cos q_2 \sin q_3 \\ 10 \sin q_2 \cos q_3 \cos q_5 - 10 \cos q_2 \sin q_5 + 20 \sin q_2 \sin q_3 \\ 10 \sin q_3 \cos q_5 - 20 \cos q_3 + 30 \end{bmatrix} \quad (47)$$

where $\mathbf{s}_{27} = [q_2 \quad q_3 \quad q_5]^T$ and

$$\xi_s = \begin{bmatrix} -10 \sin q_2 \cos q_3 \cos q_5 + 10 \cos q_2 \sin q_5 - 20 \sin q_2 \sin q_3 & -10 \cos q_2 \sin q_3 \cos q_5 + 20 \cos q_2 \cos q_3 & & & \\ 10 \cos q_2 \cos q_3 \cos q_5 + 10 \sin q_2 \sin q_5 + 20 \cos q_2 \sin q_3 & -10 \sin q_2 \sin q_3 \cos q_5 + 20 \sin q_2 \cos q_3 & & & \\ 0 & 10 \cos q_3 \cos q_5 + 20 \sin q_3 & & & \\ & -10 \cos q_2 \cos q_3 \sin q_5 + 10 \sin q_2 \cos q_5 & & & \\ & -10 \sin q_2 \cos q_3 \sin q_5 - 10 \cos q_2 \cos q_5 & & & \\ & -10 \sin q_3 \sin q_5 & & & \end{bmatrix} \quad (48)$$

For $q_2 = q_2^L = \pi/4$, $\mathbf{E}_2[\mathbf{s}_\epsilon] = \mathbf{E}_{RE}$, and applying this to $[\xi_s]^T$ yields

$$\mathbf{E}_2[\xi_s]^T = \begin{bmatrix} -5\sqrt{2} \sin q_3 \cos q_5 + 10\sqrt{2} \cos q_3 & -5\sqrt{2} \sin q_3 \cos q_5 + 10\sqrt{2} \cos q_3 & 10 \cos q_3 \cos q_5 + 20 \sin q_3 \\ -5\sqrt{2} \cos q_3 \sin q_5 + 5\sqrt{2} \cos q_5 & -5\sqrt{2} \sin q_3 \sin q_5 - 5\sqrt{2} \cos q_5 & -10 \sin q_3 \sin q_5 \\ 0 & 0 & 0 \end{bmatrix} \quad (49)$$

For a rank-deficiency of one, there are three determinants yielding analytic functions

$$D|_3 = 100(\cos q_5)^2 \sin q_3 - 200 \cos q_3 \cos q_5 = 0 \quad (50)$$

$$D|_2 = 50 \sin q_5 \sqrt{2} \cos q_5 - 50 \cos q_3 (\cos q_5)^2 \sqrt{2} - 100 \sin q_3 \cos q_5 = 0 \quad (51)$$

$$D|_1 = 50 \sin q_5 \sqrt{2} \cos q_5 + 50 \cos q_3 (\cos q_5)^2 \sqrt{2} + 100 \sin q_3 \cos q_5 = 0 \quad (52)$$

Simultaneously solving the above system of equations yields a second constant generalized coordinate $q_5 = \pi/2$ or $q_5 = 3\pi/2$ (in addition to $q_2 = \pi/4$). Therefore, the set $\gamma_1 = \{q_2 = \pi/4, q_5 = \pi/2\}$ is identified. Eleven additional sets are computed and when substituted into $\xi_{27}(\mathbf{s}_{27})$, yield parametric equations of subvarieties. For example, substituting

γ_1 into Eq. (47) yields $\kappa_1(\beta_1) = [5\sqrt{2} + 10\sqrt{2} \sin q_3 \quad -5\sqrt{2} + 10\sqrt{2} \sin q_3 \quad -20 \cos q_3 + 30]^T$; $(\pi/4) \leq q_3 \leq (5\pi/4)$, where $\beta_1 = q_3$. Substituting all second-order singularity sets into Eq. (47) yields a number of curves κ_j ; $j = 1, \dots, 12$, shown in Fig. 6a. The reducible variety whose boundaries are now established and defined by segments is shown in Fig. 6b.

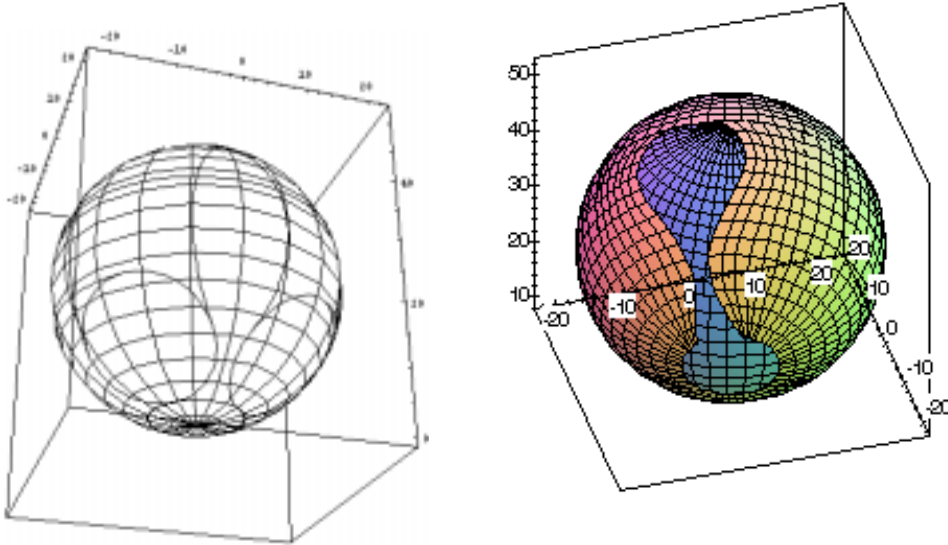


Fig. 6. (a) Subvarieties of ξ_{27} shown as curves (b) The reducible variety ξ_{27}
 The four reducible varieties due to $(\mathbf{p}_{27} \dots \mathbf{p}_{30})$ are shown in Fig. 7a. The manifold obtained by combining all varieties is shown in Fig. 7b which represents the exact material removed.

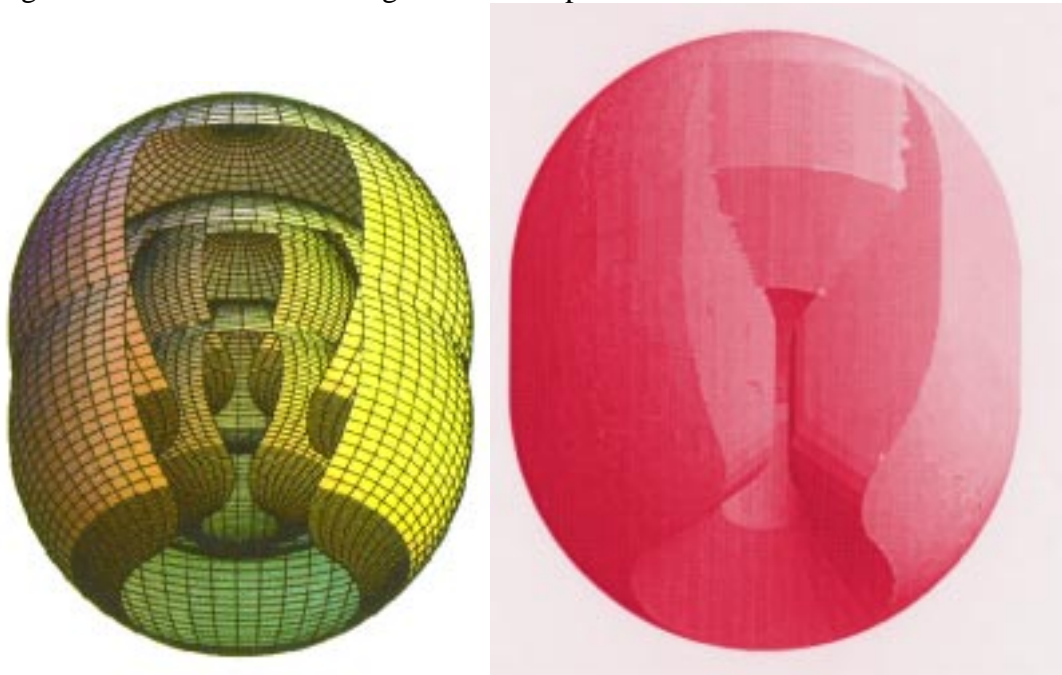


Fig. 7 (a) Four reducible varieties (b) The boundary to the manifold (material removed)

7. EXAMPLE ON COMPUTING THE VOLUME

Consider a motion of the cutting tool characterized by a curve given by the parametric vector $\Gamma(\mathbf{u}) = [5\cos u \ 5\sin u \ 1]^T$. The curve will be rotated about three axes in space given by the

rotation matrices $\mathbf{R}_i = \begin{bmatrix} \cos v_i & -0.5\sin v_i & 0.866\sin v_i \\ \sin v_i & 0.5\cos v_i & -0.866\cos v_i \\ 0 & 0.866 & 0.5 \end{bmatrix} i = 1, \dots, 3$ and the sweep vectors

$\Psi_1 = [3\cos v_1 \ 3\sin v_1 \ 1]^T$, $\Psi_2 = [4\cos v_2 \ 4\sin v_2 \ 1]^T$, and $\Psi_3 = [3\cos v_3 \ 3\sin v_3 \ 1]^T$. This operation is illustrated in Fig. 8.

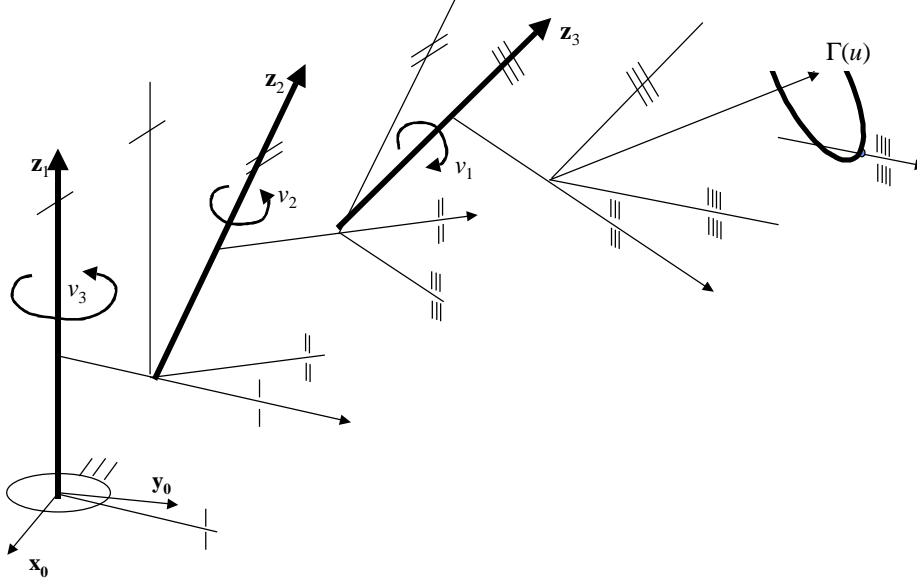


Fig. 8 A four parameter verification

Every point in the manifold is characterized by the vector function

$$\xi(\mathbf{q}) = \begin{bmatrix} c_4(c_3(c_1c_2 - 5s_1s_2) + (.75s_1 - .25c_2s_1 - .5c_1s_2s_3) + .375s_1 - .187s_{1-2}) \\ c_4(c_3(s_1c_2 + 5c_1s_2) + (-.75c_1 + .25c_2c_1 - .5s_1s_2s_3)) \\ c_4(.86c_3s_2 + (.43 + .43c_2)s_3) + (.22 - .65c_2 + 5(.43 + .43c_2)c_3 - .43s_2s_3)s_4 \\ + .5c_3(.75s_1 - .25c_2s_1 - .5c_1s_2) + .56s_{1+2} - .5(c_1c_2 - .5s_1s_2)s_3s_4 \\ + (-.375c_1 + .187c_{1-2} + .56c_{1+2} + .5c_3(-.75c_1 + .25c_2c_1 - .5s_1s_2) - .5(c_2s_1 + .5c_1s_2)s_3)s_4 \\ + 0 \end{bmatrix}$$

where c_i denotes the Cosine of q_i and s_i denotes the Sine of q_i and $[v_3 \ v_2 \ v_1 \ u] = [q_1 \ q_2 \ q_3 \ q_4]$. For this 4-parameter NC operation, the varieties are calculated by first determining the 22 singular sets. For example, the varieties at $\mathbf{p}_6 = \{q_3 = -2\pi/3, q_4 = -2\pi/3\}$ and $\mathbf{p}_7 = \{q_3 = 2\pi/3, q_4 = 2\pi/3\}$ are shown in Fig. 9.

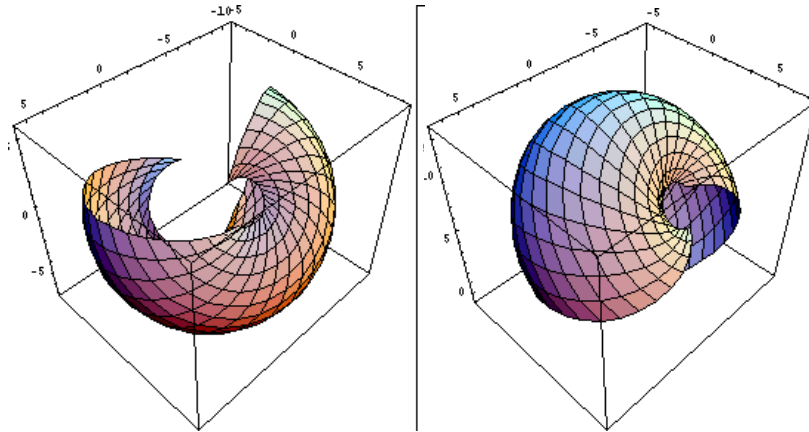


Fig. 9 Varieties due to \mathbf{p}_6 and \mathbf{p}_7

Because one can compute exact boundaries to the manifold with this formulation, it is now possible to obtain cross sections through the volume by computing the traces of each variety on a cutting plane. For example, for this machining operation, cross sectional cuts at an elevation of $z = 0.0$ and $z = 1.0$ are shown in Fig. 10.

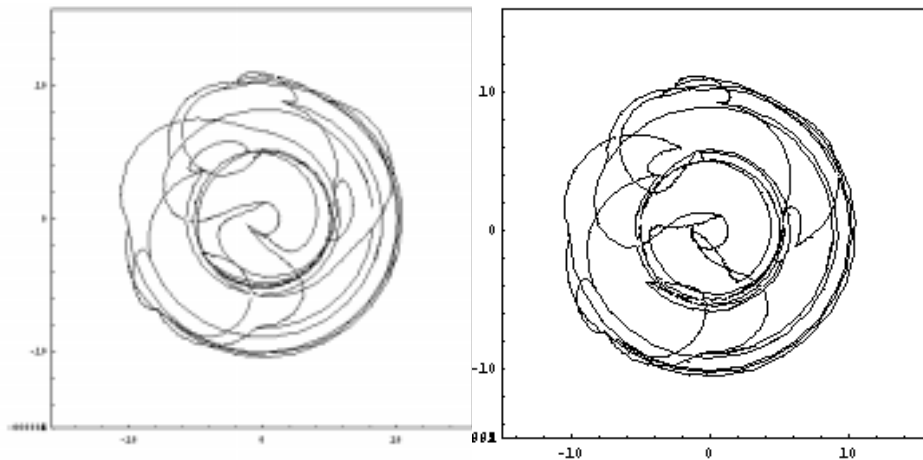


Fig. 10 (a) cross section at $z_i = 0$ (b) cross-section at $z_i = 1$

Upon identifying the boundary R_i , the area $A(R_i)$ for each cross section is computed and shown plotted in Fig. 11 for various z -elevations of the cutting plane. The volume is computed using a numerical trapezoidal integration method to be $V_{spline} = 4938 u^3$.

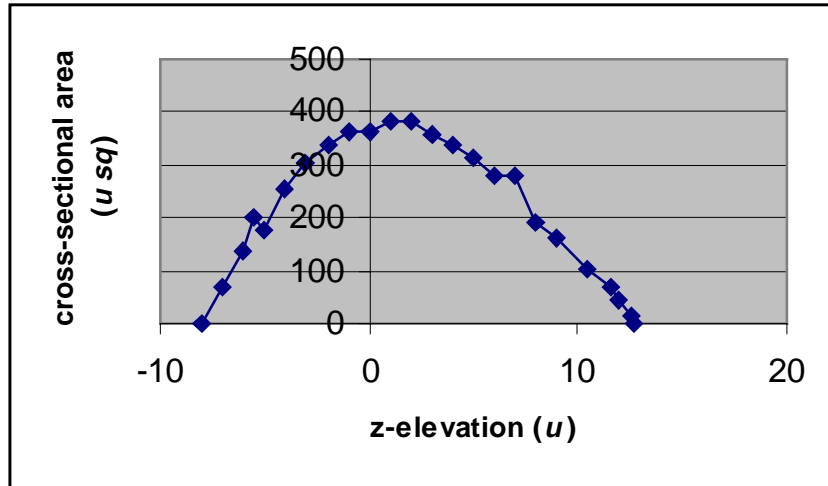


Fig. 11 Area of each cross section through the swept volume versus the z -elevation

A Note on Accuracy: The formulation for manifold stratification is exact and does not depend on any approximation. The only approximation arises in computing sections through the manifold since a numerical method is implemented to obtain traces of each variety on a cutting plane. In addition, volume computation involves a numerical integration algorithm that is inherently tolerance dependent.

8. CONCLUSIONS

A formulation for representing material removed of an up to 5-parameters machining verification process has been presented and illustrated through examples. The material removed was formulated in terms of generalized coordinates including inequality constraints imposed on the object's dimensions and sweep geometry. Inequality constraints were transformed to equality constraints and included in the analysis. It was shown that the resulting swept volume could be stratified by employing the implicit function theorem. It was observed that some varieties produced from the swept volume are characterized by a rank deficiency condition. It was also observed that these varieties can be further reduced and were able to define the boundary surface of the swept volume. While the code developed for this analysis is at an experimental stage, it is believed that this is a rigorous method for NC verification based on a broadly applicable formulation.

Also presented is a method for identifying the boundary, and voids in a swept volume. The strength of this formulations lies in the ability to simulate the verification process in terms of boundary surfaces to the simulated material removal as parametric equations, in the ability to identify the boundary, and in the ability to compute the volume of material removed by obtaining cross-sections through the manifold.

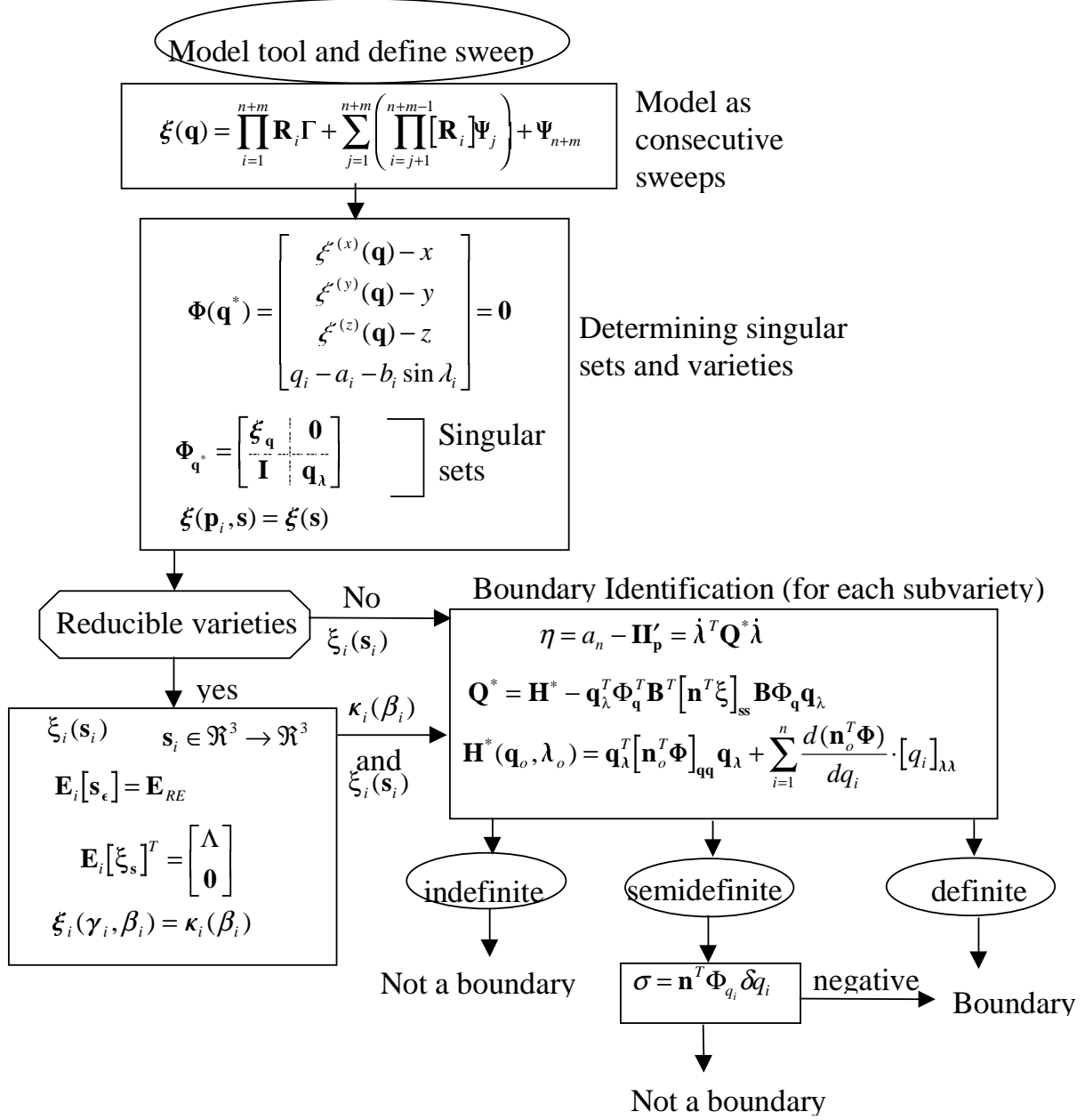
9. REFERENCES

Abdel-Malek, K and Yeh, H, 1997a "Geometric Representation of the Swept Volume Using Jacobian Rank-Deficiency Conditions," *Computer Aided Design*, Vol. 29(6), pp. 457-468.

- Abdel-Malek, K., Adkins, F., Yeh, H.J., and Haug, E.J., 1997, "On the Determination of Boundaries to Manipulator Workspaces," *Robotics and Computer-Integrated Manufacturing*, Vol. 13, No. 1, pp.63-72.
- Abdel-Malek, K., and Yeh, H.J., 1997b, "Analytical Boundary of the Workspace for General 3-DOF Mechanisms, *The International Journal of Robotics Research*, Vol. 16, No. 2, pp.1-12.
- Abdel-Malek, K., Yeh, H.J., and Othman, S., 1998, "Swept Volumes, Void and Boundary Identification", *Computer Aided Design*, Vol. 30, No. 13, pp. 1009-1018.
- Ahn, JC, Kim, MS, Lim, SB, 1997, "Approximate general sweep boundary of 2D curved object", *CVGIP: Computer Vision Graphics and Image Processing*, Vol. 55, pp. 98-128.
- Blackmore, D, Leu, MC, Wang, LP, Jiang, H, 1997, "Swept Volumes: a retrospective and prospective view," *Neural parallel and Scientific Computations*, Vol. 5, pp. 81-102.
- Blackmore, D., Leu, M.C., Wang, L.P., 1997, "Sweep-envelope differential equation algorithm and its application to NC machining verification", *Computer Aided Design* Vol. 29, No. 9, pp. 629-637.
- Blackmore, D, Leu, MC, Wang, LP, and Jiang, H, 1997, "Swept Volumes: a Retrospective and Prospective View," *Neural, Parallel, and Scientific Computations*, 5, pp. 81-102.
- Boussac, S and Crosnier, A, 1996, "Swept volumes generated from deformable objects application to NC verification", *Proceedings of the 13th IEEE International Conference on Robotics and Automation*. Part 2 (of 4) Apr 22-28, Vol. 2, Minneapolis, MN, pp. 1813-1818
- Elber, G, 1997, "Global error bounds and amelioration of sweep surfaces," *Computer Aided Design*, Vol. 29, pp.441-447.
- Farin, G., 1993, *Curves and Surfaces for Computer Aided Geometric Design*, Academic Press, San Diego, CA.
- Guillemin, V. and Pollack, A., 1974, *Differential Topology*, Prentice-Hall.
- Jerard, R and Drysdale, R 1991, Methods for geometric modeling, simulation, and spatial verification of NC machining programs", *Product Modeling for Computer Aided Design*, North Holland, Amsterdam, pp. 1-14.
- Jerard, R and Drysdale, R, 1988 'Geometric Simulation of Numerical Control Machinery' *ASME Computers Engineer* Vol 2, pp129-136.
- Koren, Y. and Lin, R.S., 1995, "Five-axis surface interpolators, *Annals of CIRP*, 44(1), 379-382.
- Leu, M C., Wang, L, Blackmore, D., 1997, "Verification program for 5-axis NC machining with general APT tools" *CIRP Annals - Manufacturing Technology* Vol. 46, No. 1, pp. 419-424
- Liang, X, Xiao, T, Han, X, Ruan, JX, 1997, Simulation Software GNCV of NC Verification, Author Affiliation: *ICIPS Proceedings of the 1997 IEEE International Conference on Intelligent Processing Systems*, Part 2 Oct 28-31, Vol. 2, Beijing, China pp. 1852-1856.
- Ling, ZK and Chase, T 1996, "Generating the swept area of a body undergoing planar motion," *ASME J. Mech. Design*, Vol 118, pp221-233.
- Liu, C, and Esterling, D, 1997, "Solid Modeling of 4-Axis Wire EDM Cut Geometry", *Computer Aided Design* Vol. 29, No. 12, pp. 803-810
- Liu, C., Esterling, D.M., Fontdecaba, J., Mosel, E, 1996, "Dimensional verification of NC machining profiles using extended quadtrees", *Computer Aided Design* Vol. 28, No. 11, pp. 845-852.
- Liu, Chonglin; Esterling, Donald, 1997, "Solid modeling of 4-axis wire EDM cut geometry", *Computer Aided Design* v 29 n 12, pp803-810.
- Lu, Y.C. "Singularity Theory and an Introduction to Catastrophe Theory", Springer-Verlag, New York, 1976

- Menon, J.P. and Robinson, D.M. 1993, "Advanced NC verification via massively parallel raycasting," *ASME manufacturing Review*, Vol. 6, 141-154.
- Menon, J.P., Voelcker, H.B. 1992, "Toward a comprehensive formulation of NC verification as a mathematical and computational problem", *Proceedings of the 1992 Winter Annual Meeting of ASME*, Nov 8-13, Vol. 59, Anaheim, CA, pp. 147-164.
- Narvekar, AP, Huang, Y, and Oliver, J, 1992, "Intersection of rays with parametric envelope surfaces representing five-axis NC milling tool swept volumes", *Proceedings of the 1992 18th Annual ASME Design Automation Conference*, Vol. 44, Scottsdale, AZ, pp. 223-230.
- Oliver, J and Goodman, E, 1990, "Direct Dimensional NC Verification" *Computer Aided Design* Vol. 22, pp. 3-9.
- Oliver, J H 'Efficient Intersection of Surface Normals with Milling Tool Swept Volumes for Discrete Three-axis NC Verification' *ASME DE* Vol 23(1) (1990) pp159-164.
- Sourin, A and Pasko, A 1996, "A function representation for sweeping by a moving solid," *IEEE Transactions on visualization and Computer Graphics*, Vol2, pp11-18.
- Spivak, M. 1968, *Calculus on Manifolds*, Benjamin/Cummings.
- Takata, S, Tsai, MD, and Inui, M, "1992, "A cutting simulation system for machinability evaluation using a workpiece model," *Annals of CIRP* 38:539-542.
- Voelker, H B and Hunt, W A, 1985, 'The Role of Solid Modeling in Machining Process Modeling and NC Verification' *SAE Tech. Paper* #810195.
- Wang, W P and Wang, K.K., 1986, "Geometric Modeling for Swept Volume of Moving Solids" *IEEE Computer Graphics and Applications*, Vol. 6, No. 12, pp. 8-17.

10. Appendix A



APPENDIX

Because the hypersurface is parametrized in three generalized coordinates, it is difficult to readily depict it. To use a commercial mathematics code, it is necessary to formulate the equation of the surface in terms of two parameters and to define parametric limits in the form of inequality constraints. It is necessary to convert the hypersurface to $\xi(\mu_1, \mu_2)$ having limits as

$$f(\mu_2) \leq \mu_1 \leq g(\mu_2) \quad (48)$$

and
$$\mu_2^l \leq \mu_2 \leq \mu_2^u \quad (49)$$

Each surface region in Fig. 7b is transformed into one that can be plotted by determining the functions $f(\mu_2)$ and $g(\mu_2)$. Define the variable μ_2 as

$$\mu_2 = (\mu_2^u - \mu_2^l)s + \mu_2^l \quad (50)$$

where the new parameter s is constrained as $0 \leq s \leq 1$. Then, the second parameter can be written as

$$\mu_1 = [g(\mu_2) - f(\mu_2)]t + f(\mu_2) \quad (51)$$

where the new parameter t is constrained as

$$0 \leq t \leq 1 \quad (52)$$

Substituting Equation (50) into Equation (51) yields the parameter μ_1 as a function of both s and t such that

$$\mu_1 = [g'(s) - f'(s)]t + f'(s) \quad (53)$$

where the primed symbol indicates the new function. Substituting Equations (50) and (53) into the parametric surface equation yields the surface equation in terms of s and t and constrained as $0 \leq s \leq 1$ and $0 \leq t \leq 1$. This final form can be directly shown using Mathematica®.

PERTURBATION METHOD TO DETERMINE THE BOUNDARY

Since hypersurfaces extend internal and external to the workspace envelope, it is necessary to identify regions (surface patches) of these hypersurfaces that are on the boundary, whether the *external boundary* or a *void*.

The curves resulting from the intersection of hypersurfaces divide each surface into many regions. An algorithm developed by the authors (Abdel-Malek and Yeh 1996, 1997c) is implemented to identify these regions whereby curves of intersection are traced. In fact, these curves represent singular trajectories of the end-effector at which the manipulator loses at least two degrees of freedom (coupled singularities). The intersection of two singular curves identify the so-called *bifurcation point*.

To determine if a region is internal, a perturbation method is employed. Consider a point \mathbf{q}^c on a hypersurface but not on the boundary, i.e., $q_i^L < q_i^c < q_i^U$. At $\xi(\mathbf{q}^c)$, the velocity of the end-effector is given by

$$[\dot{\xi}] = [\xi_{\mathbf{q}^*}] [\mathbf{q}_\lambda^*] [\dot{\lambda}] \quad (28)$$

On a singular surface, the term $[\xi_{\mathbf{q}^*} \mathbf{q}_\lambda^*] \Big|_{\mathbf{q}_o^* \lambda_o}$ is rank-deficient. Multiplying both sides of Eq. 28 by \mathbf{N}_o^T (the basis of the null space of $\xi_{\mathbf{q}^*} \mathbf{q}_\lambda^*$) yields

$$\mathbf{N}_o^T \dot{\xi} = \mathbf{N}_o^T \xi_{\mathbf{q}^*}(\mathbf{q}^c) \mathbf{q}_\lambda^* \dot{\lambda} = 0 \quad (29)$$

Since \mathbf{N}_o^T is a constant vector at \mathbf{q}^c , the left hand side of Eq. 29 characterizes the equation of a plane in \mathfrak{R}^3 as $N_1 \dot{x} + N_2 \dot{y} + N_3 \dot{z} = 0$ where $\mathbf{N}_o = [N_1 \ N_2 \ N_3]^T$ is indeed a vector **normal** to the tangent plane of the singular surface at \mathbf{q}^c . Indeed, for any value of $\dot{\mathbf{q}}$, all resulting velocity vectors $\dot{\xi}$ will lie on a plane which has \mathbf{N}_o^T as its normal. Two observations can be made:

- (i) The basis of the null space of $\left[\xi_{\mathbf{q}^*} \mathbf{q}_\lambda^* \right]^T$ is the vector normal to the singular surface at \mathbf{q}^c .
- (ii) For any given joint velocity vector $\dot{\mathbf{q}}$, the velocity of the end-effector is either tangent to the singular surface or zero, i.e., the normal component of the end-effector velocity is always zero, i.e., $v_n = \mathbf{N}_o \cdot \dot{\xi} = \mathbf{N}_o^T \dot{\xi} = 0$ (this result is reported by Haug *et al.* 1996 using a different approach).

For this normal, two points along the normal on each side of the surface can be found as

$$\xi^{p_{1,2}} = \xi(\mathbf{q}^c) \pm \mathbf{N} \partial \vartheta \quad (30)$$

where $\partial \vartheta$ is a small variation from $\xi(\mathbf{q}^c)$ (e.g., $\partial \vartheta = 0.1$). If both points ξ^{p_1} and ξ^{p_2} satisfy the constraint equation, then the region for which $\xi(\mathbf{q}^c)$ belongs is internal to the boundary.

Performing this test on all regions yields boundary surface patches defined by the equations of $\xi(\mathbf{q}^*)$ and bound by the numerical curves.

$$\Phi_{\mathbf{q}} \mathbf{q}_s \Big|_{\mathbf{q}_o, s_o}$$

NC verification software based on ray casting methods were demonstrated by (Liang, *et al.* 1997).